Nonequilibrium relaxation of a stretched polymer chain

Yu-Jane Sheng and Pik-Yin Lai*
Department of Physics, National Central University, Chung-li, Taiwan 32054, Republic of China

Heng-Kwong Tsao
Department of Chemical Engineering, National Central University, Chung-li, Taiwan 32054, Republic of China
(Received 4 March 1997; revised manuscript received 17 April 1997)

The static and nonequilibrium dynamic properties of a single linear polymer chain under a traction force f is studied by Monte Carlo simulations using a continuous model and by scaling calculations. Chain lengths from $N=10$ to 100 are considered. For the static results, our simulation data show that the averaged end-to-end distance $\langle R_f\rangle \sim N^{2\nu} f$ at weak tension forces and for strong forces $\langle R_f\rangle \sim N f^{1/\nu-1}$, which are consistent with previous studies. The nonequilibrium relaxation behavior is studied for an initially stretched polymer chain, when the stretching force is removed. Detail chain configurations during the relaxation process are analyzed from the simulation data. Different relaxation dynamics are found for three regions: the linear, Pincus, and model-dependent regimes. The nonequilibrium relaxation time τ is derived in the linear ($\tau \sim N^{1+2\nu}$), Pincus ($\tau \sim N^2 f^{1/\nu-2}$), and model-dependent regimes. These results are compared with our Monte Carlo data and recent experiments, and are discussed in the light of scaling theories. [S1063-651X(97)04508-X]

PACS number(s): 61.41.+e, 05.70.Fh

I. INTRODUCTION

The study of static and dynamic properties of a single polymer chain is the key to the understanding of many polymeric materials. Recently, Perkins and co-workers [1,2] were able to visualize a single tethered DNA molecule under flows. The DNA molecule was stretched to full elongation and the relaxation behavior was observed as the flow stopped. Their results were interpreted in terms of the Zimm model [3], in which the longest relaxation time $\tau \sim N^{3\nu}$, and 3ν ranges from 1.53 to 1.79 depending on the variation of chain lengths. This work inspires many continuing theoretical studies [4–8]. However, as pointed out in Ref. [4], DNA's structure is quite special, with a large persistence length, and a fully elongated double helix structure may have a different controlling factor in the stretch-coil transformations. Also, both static and dynamic properties behave somewhat nonuniversally under strongly stretched conditions. Thus it is of great importance to study a simple polymer coil under different stretching forces to understand this interesting phenomenon.

de Gennes and Pincus [9,10] performed some pioneering studies on the static properties of deformed, isolated, flexible polymers in the limit of weak and strong forces, respectively. Webman, Lebowitz, and Kalos [11] were the first to observe the weak force regime and the Pincus scaling through computer simulation. Wittkop *et al.* [12] extended the description of the deformation behavior over the full force range by using the scaling function obtained from renormalization-group studies. They also performed computer simulations using the bond fluctuation model to find the relationship between the projection of the end-to-end vector in the force direction as a function of the applied force. However, the more difficult problem concerning the dynamical behavior is less studied. According to Pincus [13], for a small fluctuation about the distorted equilibrium position for chains under traction forces, the fundamental relaxation time has the expression $\tau_{\rm eq} \sim R_F^{2/\nu} f^{(2-3\nu)/\nu}$, where R_F is the Flory radius and f is the stretching force. This means that in good solvents ($\nu \approx \frac{3}{5}$) the relaxation time increases as f increases. Another similar situation is also of interest where the observation of the relaxation behavior proceeds under the condition that the applied force on the chain is removed at $t=0$. This relaxing process has not been studied in detail in either computer simulations or theoretical work. Much interest therefore remains in obtaining the nonequilibrium dynamical behavior of a deformed, isolated polymer chain. In this paper, we perform Monte Carlo simulations and scaling calculations to investigate the static and dynamic behaviors of a single polymer chain in good solvents. The polymers are simulated in a continuous space. As pointed out by Binder and Paul [14], the elementary move of the Monte Carlo process must be carefully chosen so that it corresponds to actual motions in a coarse-grained sense. It is generally accepted that the ability of the algorithm to generate Rouse dynamics in the free-draining limit is the test of the algorithm.

The plan of this article is as follows. Section II is a brief review of the static properties of a single chain under traction. Then in Sec. III the scaling expressions of the nonequilibrium relaxation times for a stretched chain are calculated using an elastic model picture as the external force is removed at $t=0$ in three different regimes. In Sec. IV, the simulation model and method are introduced. Section V contains the static and equilibrium results of the Monte Carlo simulations. The data for the nonequilibrium relaxation upon releasing a stretched chain are given in Sec. VI. Section VII contains comparisons made between Monte Carlo simulation data, the scaling analyses, and recent experiments, as well as some outlooks.

*Author to whom all correspondence should be addressed. Electronic address: pylai@phyast.phy.ncu.edu.tw

II. BRIEF REVIEW IN STATIC PROPERTIES

According to Pincus [10], a single polymer chain under an external force f has two characteristic lengths: the Flory radius R_F and the tensile screening length ξ. $R_F = aN^{\nu}$, where N is the number of monomers in the chain, a is the monomer size, and $\nu \approx \frac{3}{5}$ in good solvent conditions. The blob size is related to the temperature T via $\xi = k_B T/f$, where k_B is the Boltzmann factor. The cases of weak and strong forces correspond to the $R_F/\xi \ll 1$ and $R_F/\xi \gg 1$ conditions, respectively. The average end-to-end displacement in the force direction of a chain under a constant force f, $\langle R_f \rangle$, can be written in a scaling form as

$$\langle R_f \rangle = R_F \Phi(R_F/\xi), \tag{1}$$

where $\Phi(x)$ is a dimensionless scaling function. For small f, we expect R_f to be linear in f, and thus $\Phi(x \to 0) \cong x$. Therefore in the limit of weak force, the polymer coil has a restoring force as

$$\langle R_f \rangle \sim \frac{f}{k_B T} R_F^2 = N^{2\nu} a \mathcal{F}, \tag{2}$$

where the dimensionless reduced force $\mathcal{F} \equiv fa/(k_B T)$ is introduced for convenience. Note that $\langle R_f \rangle$ is nonlinear in N at low forces for chains under traction in good solvents. In the ideal case ($\nu = \frac{1}{2}$), the tension force is transmitted along the backbone, while for chains in good solvent conditions, the transmission is also through contacts between certain pairs of monomers due to excluded volume interactions [3].

For a chain under an external force such that the resulting end-to-end extension exceeds the Flory radius R_F but does not yet become comparable to the fully extended length Na (the Pincus regime), $\Phi(x)$ is assumed to be proportional to x^p where p can be determined by the condition $\langle R_f \rangle \sim N$, which gives $p = 1 - 1/\nu$. The same expression can also be obtained according to the blob theory: At strong enough f, the chain breaks up into an ideal string of noninteracting blobs (as shown in Fig. 1), each with size $\xi = ag^{\nu}$, where g is the number of monomers in a blob. The end-to-end extension can be estimated as follows:

$$\langle R_f \rangle \simeq (N/g)\xi = (a/\xi)^{1/\nu} N \xi = R_F^{1/\nu} \xi^{1-1/\nu}. \tag{3}$$

As mentioned earlier, in the Pincus regime $\xi = k_B T/f$, and thus the stress-strain relationship gives

$$\langle R_f \rangle \sim R_F^{1/\nu} \left(\frac{f}{k_B T} \right)^{(1/\nu)-1} = Na \mathcal{F}^{(1/\nu)-1} \tag{4}$$

In good solvents, where $\nu \approx \frac{3}{5}$, $\langle R_f \rangle \propto f^{2/3}$, instead of the linear Hooke's law as in Eq. (2). It is worth mentioning that for extremely strong f (beyond the Pincus regime), $\langle R_f \rangle$ becomes comparable to aN, and the stress-strain relation for the chain is dominated by short-range monomer-monomer interactions, which result in a nonuniversal behavior.

Apart from the longitudinal elongation (parallel to f), it is of interest to study the square of the lateral spread of the chain, $\langle R_{\text{perp}}^2 \rangle$. In linear regime, $\langle R_{\text{perp}}^2 \rangle$ remains roughly undisturbed. However, according to the blob pictures, in the Pincus regime, $\langle R_{\text{perp}}^2 \rangle$ scales as $(N/g)\xi^2$, and thus the cross section diminishes as

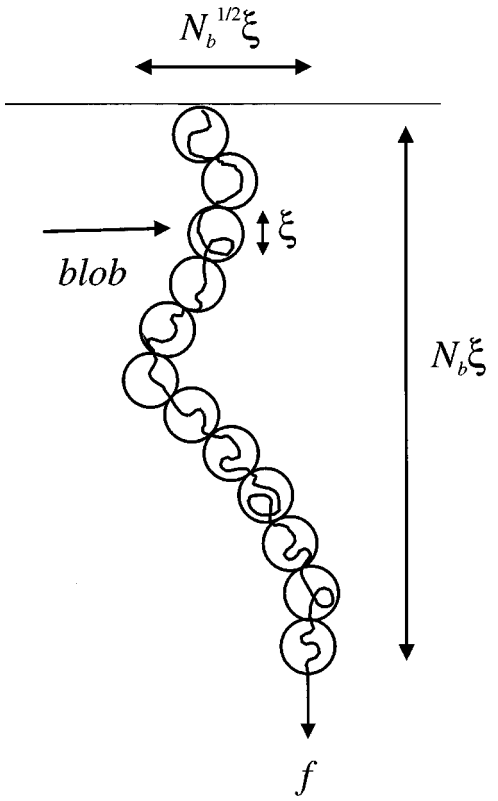

FIG. 1. Schematic blob picture of polymer chain stretched by a force f at its end. ξ is the blob size and $N_b = N/g$ is the number of blobs in the chain.

$$\langle R_{\text{perp}}^2 \rangle \cong R_F^{1/\nu} \left(\frac{k_B T}{f} \right)^{2-(1/\nu)} = Na^2 \mathcal{F}^{1/\nu - 2}. \tag{5}$$

As can be seen, in good solvents where $\nu \approx \frac{3}{5}$, the chain not only elongates but also shrinks in its lateral dimensions under strong elongation. These results together with Eqs. (2) and (4) indicate that volume of the stretched chain varies with the force as $V \sim f$ and $V \sim f^{-3+2/\nu} \sim f^{1/3}$ in the linear and Pincus regimes, respectively. Thus in the Pincus regime, the structure of a stretched chain can be viewed as (see Fig. 1) an ideal random walk of blobs: in the force direction, it is a biased ideal random walk (thus $R_f \propto N/g$), while it is an unbiased random walk in the lateral direction (thus $R_{\text{perp}} \propto \sqrt{N/g}$).

III. SCALING ANALYSIS OF DYNAMIC PROPERTIES

Pincus [13] also studied the dynamics of a stretched polymer chain including both excluded volume effects and hydrodynamic interactions in the strongly stretched regime. By balancing the elastic restoring force and viscous drag for small fluctuations about the distorted equilibrium conformations, the fundamental renormalized relaxation time has been found to be

$$\tau_{\text{eq}} \simeq \frac{6\pi\mu}{k_B T} R_F^{2/\nu} \xi^{3-2/\nu}, \tag{6}$$

where τ_{eq} is the equilibrium relaxation time of the chain under a constant force, μ is the viscosity, and $\xi(=k_BT/f)$ is the Pincus blob size. For good solvent conditions, $\tau_{eq}\sim f^{2/\nu-3}\sim f^{1/3}$.

However, in this work we are interested in the case where the polymer chain is initially stretched and allowed to equilibrate under the constant stretching force, and then the nonequilibrium relaxation behavior, after this stretching force is removed, is investigated. Such a nonequilibrium relaxation behavior can be analyzed by a similar method to that in Ref. [13]. The nonequilibrium relaxation process proceeds in three different regimes, as analyzed in the following.

A. Linear regime

In the linear regime where f is small, the relationship between the force and deformation in the direction of force obeys Hooke's law. The elastic restoring force f_{el} can be expressed as

$$f_{el}\sim(k_BTR_f)/R_F^2. \tag{7}$$

The work done by the external stretching force can be estimated as

$$W_{el}=\int_0^{R_o} f_{el}dR_f\sim\frac{k_BT}{R_F^2}R_o^2, \tag{8}$$

where $R_o=R_f(t=0)$. This work is dissipated by the viscous damping force which can be estimated using the Stokes' law and the Rouse model that all monomers experience the damping. The Rouse model is expected to be correct in our Monte Carlo simulation in which no hydrodynamic interaction is taken into account. Thus we obtain the viscous damping force,

$$f_v\simeq 6\pi\mu a(\partial R_f/\partial t)N, \tag{9}$$

where μ is the viscosity. Assuming the relaxation time is dominated by a single time scale τ, the time dependence of $R_f(t)$ can be written as $R_f(t)=R_oF(t/\tau)$ for some function F. Thus the work dissipated is given by

$$W_v=\int_0^{R_o} f_vdR_f\sim\mu aN\frac{R_o^2}{\tau}. \tag{10}$$

Equating Eqs. (8) and (10), the nonequilibrium relaxation time can be estimated as

$$\tau\approx\frac{\mu a}{k_BT}NR_F^2=\frac{\mu a^3}{k_BT}N^{1+2\nu}. \tag{11}$$

This result is identical to that of de Gennes which is based on the balance between the elastic restoring force and the viscous drag for small fluctuations about the distorted equilibrium conformation. The most important outcome of this analysis is that τ is independent of the force in the linear regime. This indicates that, as expected from linear-response theory, the relaxation mechanisms are the same in both the linear region and at equilibrium.

B. Pincus regime

From Eq. (4), the restoring force in the Pincus regime is given by

$$f_{el}=(k_BT/R_F)(R_f/R_F)^{\nu/(1-\nu)}, \tag{12}$$

and the corresponding work done is

$$W_{el}\sim\int_0^{R_o} f_{el}dR_f\sim k_BT(R_o/R_F)^{1/(1-\nu)}. \tag{13}$$

Again, this work is dissipated by the viscous damping force as before,

$$f_v\simeq 6\pi\mu a(\partial R_f/\partial t)N. \tag{14}$$

However, in this regime the polymer chain is stretched, and thus hydrodynamic screening is not that important; one expects the Rouse model assumption of all monomers experience the damping to be more correct, even in the experimental situation. Assuming that $R_f=R_oF(t/\tau)$, as before, and $W_v=\int_0^{R_o}f_vdR_f$, we estimate τ to be

$$\tau\sim\frac{\mu a}{k_BT}NR_F^{1/1-\nu}R_o^{(1-2\nu)/(1-\nu)}. \tag{15}$$

Using $\mathcal{F}\equiv fa/(k_BT)$, from Eq. (4) we obtain

$$R_o=R_f(0)\approx Na\mathcal{F}^{(1/\nu)-1}. \tag{16}$$

Thus

$$\tau\approx\frac{\mu a^3}{k_BT}N^2\mathcal{F}^{(1/\nu)-2}. \tag{17}$$

Hence, in good solvents, $\tau\sim N^2f^{-1/3}$, which means that as the external force increases, the relaxation time decreases. This result is in contrast with the equilibrium relaxation time $\tau_{eq}\propto f^{1/3}$ in Eq. (6), derived with the blob picture for a constant stretching force. The major difference in these two results arises from the nonequilibrium nature in the releasing process. In the present situation, the main assumption in the blob picture, $f\xi=k_BT$, no longer holds during the relaxation process due to the fact that, in this fast process, the system cannot achieve thermal equilibrium. However, in our derivation of Eq. (13), we used the Pincus force law Eq. (12), here the building up of the elastic work done W_{el} is assumed to be in a quasistatic manner, so that Eq. (12) still holds. Then this work is dissipated in the fast nonequilibrium process of abruptly releasing the chain at $t=0$.

C. Model-dependent regime

If the initial stretching force is further increased beyond the Pincus regime, the polymer chain approaches its fully unfolded limit, and the actual bonding potential between successive monomers become important in determining the force law. As a result, the force law becomes dependent on the chemical details of the monomers and the chemical bondings; hence the force law would be nonuniversal and model dependent. However, one can still obtain some feeling about the behavior in this regime by considering some particular model. In order to allow for further analysis, we shall em-

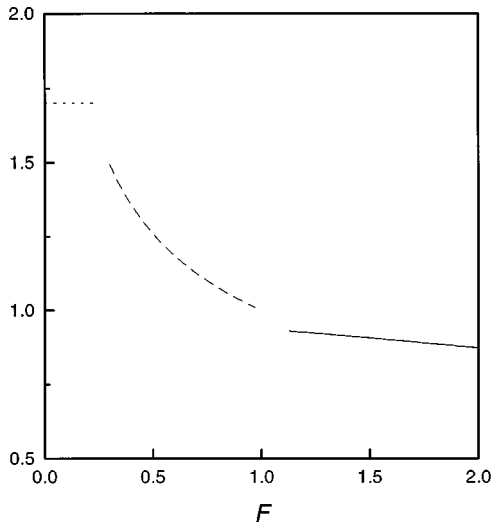

FIG. 2. Nonequilibrium relaxation time as a function of the scaled force, $\tau k_B T/(\mu N^2 a^3)$ vs $\mathcal{F}$, in the linear regime (dotted line, independent of $\mathcal{F}$), the Pincus regime [dashed curve, from Eq. (17)] and the model-dependent regime [solid curve, from Eq. (20) using the freely jointed chain model].

ploy the simple freely jointed chain model to estimate the nonequilibrium relaxation time. Furthermore, in this ultrahighly stretched regime, the polymer chain is stretched near to its saturation, and the inverse Langevin force law of the freely jointed chain would be expected to give a reasonable picture, at least qualitatively. The force law in this case is given by

$$\mathcal{F} \equiv \frac{fa}{k_B T} = \mathcal{L}^{-1}(\eta), \tag{18}$$

where $\mathcal{L}(x) = \coth x - 1/x$ is the Langevin function, and $\eta \equiv R_o/(Na)$ is the reduced end-to-end distance. In this case the elastic work done stored is given by

$$W_{\rm el} = N k_B T \int_0^{\eta} \mathcal{L}^{-1}(u)\, du. \tag{19}$$

Following the same calculation as in previous regimes, one arrives at

$$\tau \approx \frac{\mu a^3}{k_B T} N^2 \left(\frac{\eta^2}{\eta \mathcal{F} + \ln[\mathcal{F}/\sinh \mathcal{F}]} \right), \tag{20}$$

where $\eta = \mathcal{L}(\mathcal{F})$. In the extremely strong force limit $\mathcal{F} \gg 1$ and $\eta \approx 1$, one has

$$\tau \approx \frac{\mu a^3}{k_B T} N^2 \left(\frac{1}{\ln \mathcal{F}} \right). \tag{21}$$

The behavior of τ as a function of the force is shown in Fig. 2. Note that in both the Pincus regime and the model-dependent regime, τ decreases as f increases.

IV. MODEL AND SIMULATION DETAILS

The polymer chain studied in this work is modeled as beads connected by stiff springs. Previous simulations [15–17] have been very successful in exploring the phase equilibrium behavior of pure polymers and polymer-solvent solutions. The interactions between the nonbonded beads are through the standard Lennard-Jones potentials

$$U_{nb} = 4\varepsilon \left[\left(\frac{\sigma}{r} \right)^{12} - \left(\frac{\sigma}{r} \right)^{6} \right], \tag{22}$$

where ε and σ are the energy and size parameters, respectively. The monomeric ε and σ are units used for the reduced quantities for temperature and distances as $T^* = kT/\varepsilon$ and $R^* = R/\sigma$. The interactions between bonded beads are represented by a cutoff harmonic spring potential as

$$U_b = \tfrac{1}{2} k (r - \sigma)^2, \quad 0.5 < \frac{r}{\sigma} \leqslant 1.5. \tag{23}$$

The potential is infinite elsewhere. We have chosen $k\sigma^2/\varepsilon = 400$.

The systems studied contain a single polymer chain with chain length N ranging from 10 to 100. Note that the Pincus regime is defined in the range $N^{\nu} a < R_f \ll Na$, which can be quite narrow for short chains. Periodic boundary conditions are imposed in all three directions. The simulations are performed under the conditions of constant temperature, volume, and total number of beads. According to a previous study [15], the reduced θ temperature for the pure bead-spring chain is about $kT/\varepsilon = 4.59$. In the present study, the reduced temperature $T^* = 6$ is chosen so that the system is in the good solvent regime.

The initial configurations are generated by growing the chain to the desired length in a way similar to the configurational-biased insertion method [18,19]. The trial moves employed for chains are bead displacement motions [15], which involve randomly picking a bead and displacing it to a new position in the vicinity of the old position. The distance away from the original position is chosen with the probability that the condition of equal sampling of all points in the spherical shell surrounding the initial position must be satisfied. The new configurations resulting from this move are accepted according to the standard Metropolis acceptance criterion [20]. To simulate the stretching force in the $-\hat{z}$ direction, the first bead is fixed in the space, while the end bead is under an external potential $U = f z_N$, where z_N is the z coordinate of the end bead. Runs for the same chain length at different stretching forces are performed starting with the final configuration from a previous stretching force and are equilibrated for about 10^7 Monte Carlo steps (MCS). Measurements of static properties such as end-to-end distance are taken over a period of $(1–4)\times 10^6$ MCS/monomer.

The mean end-to-end distance parallel and perpendicular to the direction of the stretching force are given by

$$\langle R_f \rangle = \langle z_N - z_1 \rangle, \tag{24}$$

$$\langle R_{\rm perp}^2 \rangle = \langle (x_N - x_1)^2 + (y_N - y_1)^2 \rangle, \tag{25}$$

where (x_i, y_i, z_i) are the coordinates of the ith monomer in the chain. The angular brackets $\langle\ \rangle$ denote the ensemble average.

The equilibrium relaxation time τ_{eq} is obtained through measurements of the time correlation function for the radius of gyration defined as

$$C(t)=\frac{\langle R_g(t)R_g(0)\rangle-\langle R_g\rangle^2}{\langle R_g^2\rangle-\langle R_g\rangle^2}. \tag{26}$$

Time is measured in units of Monte Carlo steps per monomer (MCS/monomer), one MCS/monomer means that on average every monomer has attempted to move once. On the other hand, the nonequilibrium dynamical process of releasing the stretched chain at $t=0$ is characterized by the time dependence of the normalized z component of the radius of gyration $R_{gz}(t)/R_{gz}(0)$, where $R_{gz}(0)$ the radius of gyration of the z direction at $t=0$. In our simulations, this quantity is averaged over many different realizations of the releasing processes, and this average quantity is denoted by $\overline{R_{gz}(t)/R_{gz}(0)}$. Typically, this average is taken for 100–1000 realizations in our simulations.

V. EQUILIBRIUM RESULTS

As mentioned before, de Gennes and Pincus used a scaling analysis, and obtained scaling laws for the static properties of deformed chains. Webman, Lebowitz, and Kalos [11] and Wittkop *et al.* [12] performed computer simulation on lattice models to verify those scaling laws [as in Eqs. (2) and (4)]. Here we perform simulations for the static quantities in continuous space using the bead-spring chain model, thus explicitly verifying the universality of these scaling laws. In Fig. 3 the scaled mean end-to-end vector $\langle R_f\rangle/N^{\nu}$ is plotted as a function of fN^{ν} for various chain lengths. As we can see, deformation of the chain obeys Hooke's law in spite of the fact that for weak forces the statistical fluctuations are large. Also, it is quite clear that long chains reach the scaling law at weaker forces. This is because the elastic modulus is small for long chains, and thus long chains are very susceptible to external forces. The width of the crossover regime between linear and Pincus behavior is quite narrow, as pointed out in Ref. [12]. For strong forces, the Pincus expression applies, and the elastic response is significantly more nonlinear. The scaling law breaks down for very strong forces, where the chain is near to fully stretched and the deformation behavior becomes model dependent. The variation of the lateral spread of the chain $\langle R_{perp}^2\rangle$ is shown as a function of f in Fig. 4. In the linear regime, $\langle R_{perp}^2\rangle$ remains roughly constant, while, in the Pincus regime, the cross section diminishes as $f^{-2+1/\nu}\approx f^{-1/3}$. Thus our results verify the scaling law proposed by Pincus [10]. To test the reliability of our algorithm for the dynamical properties of real polymer systems, we first perform the study of the dependence of the equilibrium relaxation time for chain length with $N=5-30$ under no external force. The time autocorrelation function in Eq. (26) is measured, and the equilibrium relaxation time τ_{eq}^{o} (with $f=0$) is then extracted by assuming $C(t)\propto\exp(-t/\tau_{eq}^{o})$. We expect that the chain should follow the Rouse dynamics and the relaxation time should scale as $\tau_{eq}^{o}\sim N^{1+2\nu}$. Paul *et al.* [21] and Lai [22] have performed dynamic Monte Carlo simulations using the bond fluctuation model, and obtained $1+2\nu\approx 2.24$ and 2.18, respectively. Figure 5 shows our simulation data of the equilibrium relaxation time τ_{eq}^{o} versus chain length N. The result indicates a power law $\tau_{eq}^{o}\propto N^{1+2\nu}$, with $1+2\nu\approx 2.25$. This result is compatible with Gerroff *et al.*'s work [23] ($1+2\nu\approx 2.3$), which was done also in continuous space for a bead-spring model with soft Lennard-Jones repulsion. It is worth mentioning that the correlation function $C(t)$ is rather noisy, and it is very time consuming to obtain a smooth decay curve of $C(t)$ for long chains.

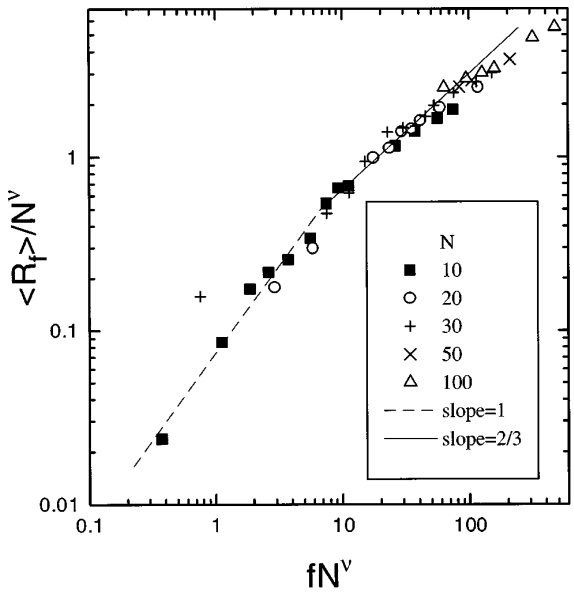

FIG. 3. Scaled end-to-end vector vs the scaled stretching force for various chain lengths as suggested in Eq. (3). Solid and dashed lines denote slopes of 1 and 2/3.

VI. NONEQUILIBRIUM RELAXATION

When the stretching force is released at $t=0$, the chain starts to relax toward the Flory coil conformation. The con-

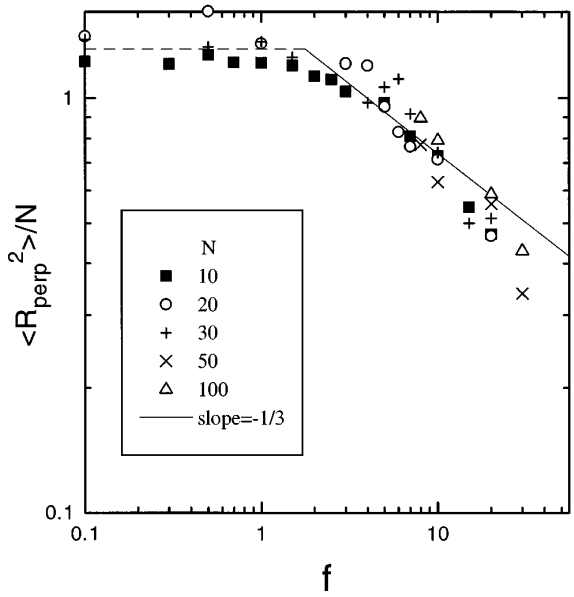

FIG. 4. $\langle R_{perp}^2\rangle/N$ vs stretching force for various chain lengths. In the weakly stretched regime, $\langle R_{perp}^2\rangle/N$ is roughly constant, while in the strongly stretched regime it diminishes as $f^{-1/3}$.

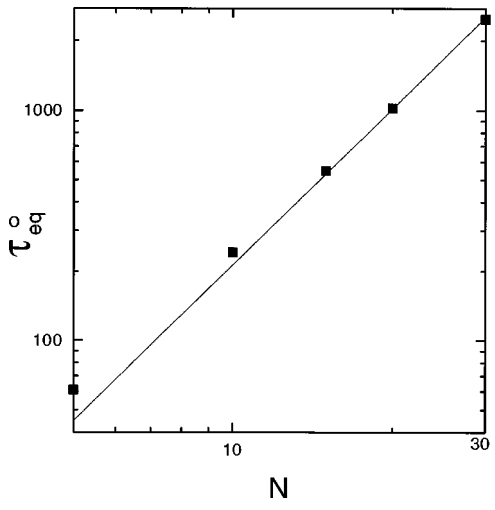

FIG. 5. Log-log plot of the equilibrium relaxation time (in units of MCS/monomer) of a chain under no external force τ_{eq}^{o} vs the chain length N.

formations of the polymer chains can be probed by looking at snapshots of their configurations during the relaxation process. As shown in Fig. 6(a), the resulting plot (in the x-z plane) greatly resembles the experimental pictures shown in Perkins *et al.*'s work. Initially the chain is stretched to a large extension. An initial rapid recoil is observed here. This phenomena can also be seen from the experiment in Ref. [24] for the static force measurement of elongated DNA under magnetic forces, which showed a highly nonlinear dependence of the force on length at $>75\%$ extensions. During this relaxation process, only small-scale internal relaxation occurs inside the stretched chain. Large-scale conformation change proceeds only from the free end. After a certain time, a portion of the chain near the free end relaxes roughly to the unperturbed state, while other parts of the chain still remain in different degrees of the stretched structures. At this stage, the tension along the chain is nonuniform. This ''unperturbed'' end portion of the chain behaves in a similar way to the Flory coil. This may explain why, in experiments by Perkins *et al.*, a ''compact ball'' was observed at the free end. Figure 7 shows the chain conformations at two different times. Before releasing ($t=0$), the chain is at the equilibrated stretched state. At $t=8$ the upper part which is near the fixed end of the chain remains in stretched form, while the lower part of the chain coils back into a roughly spherical shape. This behavior is related to rebounds in the relaxation process. The free end moves quite freely in its surrounding, and it is possible that it moves back and forth from the equilibrium position. Thus the length of the chain in the z direction fluctuates. However, the average over many relaxation processes still reveals a smoothly decaying curve (as will be shown in Fig. 9). The dynamical pictures of the described relaxation processes can be best understood from Fig. 8, in which the monomer density along the force direction ($-\hat{z}$) at different times is shown. At $t=0$ the monomer density is nearly uniform along the force direction. Upon removing the external force, the free end starts to relax. As mentioned above, the portion near the free end behaves like the Flory coil after a certain time, and the conformation change fluc-

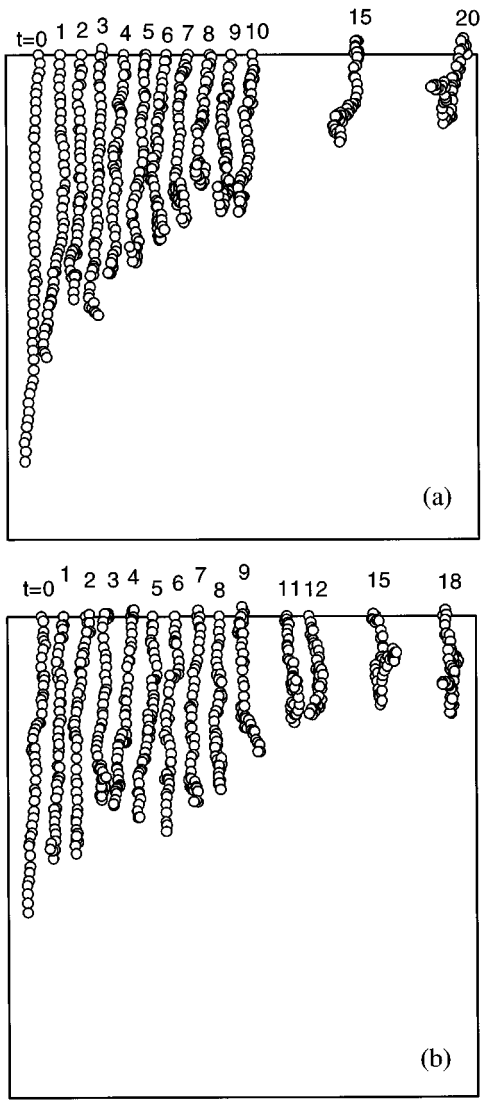

FIG. 6. Snapshots of the configurations of a single polymer chain ($N=50$) during the relaxation process. Initially the chain is stretched to a large extension with (a) $f=30$ and (b) $f=10$. The stretching force is removed at $t=0$. Snapshots between t and $t+1$ contains 7×10^4 MC steps.

tuates rather significantly. The sections with large monomer density at the chain end are consistent with the ''compact balls'' observed in the experiment by Perkins *et al.*

For nonequilibrium relaxation time studies of the releasing of a stretched chain, $R_{gz}(t)$ as a function of t, after the force f is removed at $t=0$, is monitored. Figure 9 shows the variation of $\overline{R_{gz}(t)/R_{gz}(0)}$ versus for $N=30$ under different stretching forces. These curves show the evolution of the averaged relaxation processes as the external force is removed from the chain. It can be seen that the curves become less noisy as the force increases. A smooth curve for $\overline{R_{gz}(t)/R_{gz}(0)}$ can be obtained with fewer numbers of processes for averaging as the stretching forces increase. At weak forces, $\overline{R_{gz}(t)/R_{gz}(0)}$ can be roughly fitted to an exponential decay. On the other hand, $\overline{R_{gz}(t)/R_{gz}(0)}$ is indescribable by a single exponential decay at strong forces, and decays considerably more slowly than a simple exponential

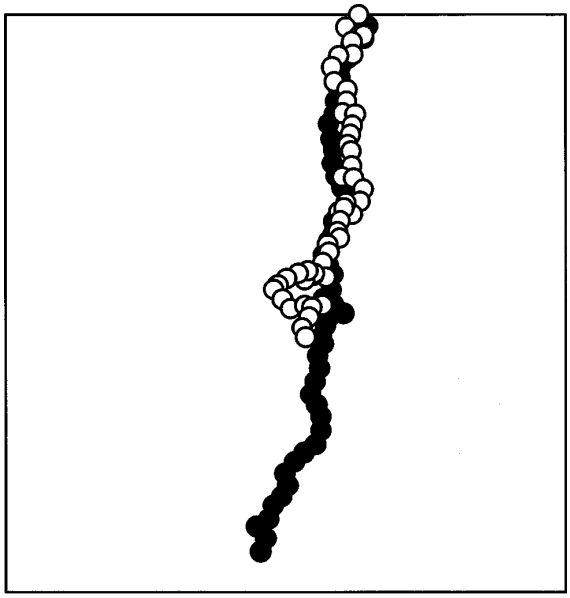

FIG. 7. Chain conformations at $t=0$ and $t=8$ for $N=50$ at $f=10$. At $t=0$ (●), the chain is at the stretched state. At $t=8$ (○), the lower part which is near the free end of the chain coils back into a ball shape.

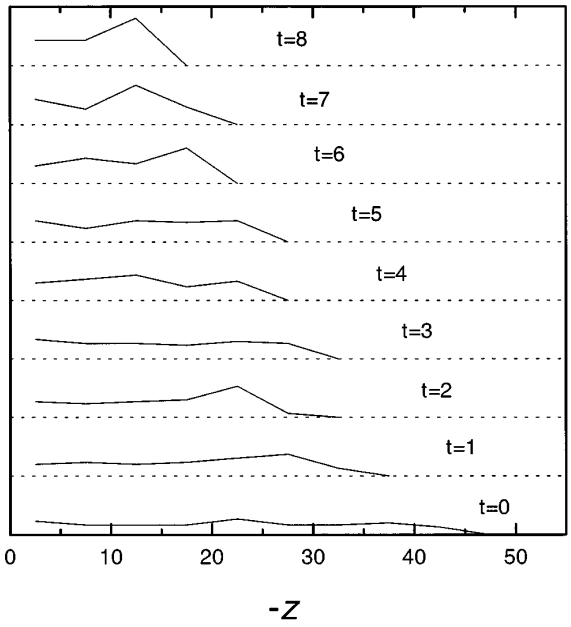

FIG. 8. Monomer density along the force direction $(-\hat{z})$ at different times for $N=50$ at $f=10$. At $t=0$, the monomer density is nearly uniform. After removing the stretching force $(t>0)$, the portion near the free end relaxes to a Flory coil after a certain time, and the conformation change fluctuates rather rapidly. Data between t and $t+1$ contain 7×10^4 MC steps.

decay. It is worth mentioning that although the averaged $\overline{R_{gz}(t)/R_{gz}(0)}$ is a monotonously decaying curve, rebounds in R_f are observed in many single realizations of the releasing processes such as one shown in Fig. 6(b) at around $t=3-6$. This phenomenon was also observed in Perkins *et al.*'s experiment, but only briefly mentioned, and no explanation was offered. We found that the rebound is less obvious if the chain is stretched with stronger forces as in Fig. 6(a).

The nonequilibrium relaxation time τ is extracted from the data of $\overline{R_{gz}(t)/R_{gz}(0)}$ by assuming it decays to $R_{gz}(\infty)/R_{gz}(0)$ as $e^{-t/\tau}$. Figure 10(a) shows the variation of τ of a single deformed chain versus f through dynamic Monte Carlo simulations and scaling analysis. We can see there are three regions: the weak-force (linear) regime, the stretched (Pincus) regime, and the model-dependent regime. As mentioned in Sec. III, in the weak-force regime the system is not far from the thermodynamic equilibrium state. The driving force for the relaxation process is the same as that in the equilibrium state (with or without a constant stretching force). Thus we expect the relaxation time to remain constant in the linear regime. Pincus [13] also used a scaling analysis to estimate the equilibrium relaxation time under a constant force f, $\tau_{\rm eq}$. His analysis showed that for the weak-force linear region, $\tau_{\rm eq}$ is independent of f. Due to the strong fluctuations, it is very difficult to obtain reliable data for τ from the decay of $\overline{R_{gz}(t)/R_{gz}(0)}$ for relatively weak forces. Instead we perform simulations to measure the auto correlation function $C(t)$ from Eq. (26), and extract $\tau_{\rm eq}$, for $N=10$ to illustrate our points. Indeed as can be seen from Fig. 10(a), the relaxation time is essentially constant in the linear regime. In the crossover regime, the system becomes weakly disturbed, and it takes a longer time for the system to relax back to the equilibrium state. The relaxation time reaches a maximum around the beginning of the Pincus regime, and then decreases as f increases with the scaling power as $\tau\sim f^{-2+1/\nu}$. These results are consistent with our scaling analysis in Eq. (17). It should be noted that τ in the linear regime is not always smaller than in the Pincus regime. In fact from Eqs. (11) and (17), these two times are of the same order if $N\approx\mathcal{F}^{-1/\nu}$. Therefore τ in the linear regime can be greater than in the Pincus regime for a sufficiently long chain. The dependence of $\tau\propto N^2$ as predicted in Eqs. (17)

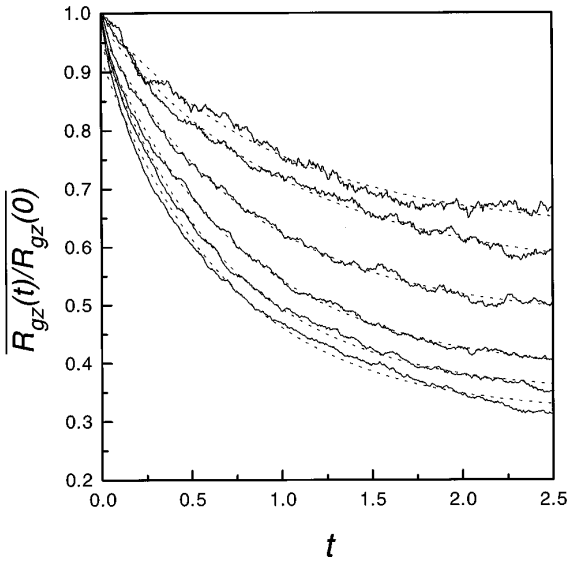

FIG. 9. $\overline{R_{gz}(t)/R_{gz}(0)}$ for $N=30$ under different stretching force (t in units of 10^6 MCS/monomer). $f=3$, 4, 7, 10, 15, and 20 from top to bottom. Dashed curves are fittings to exponential decays.

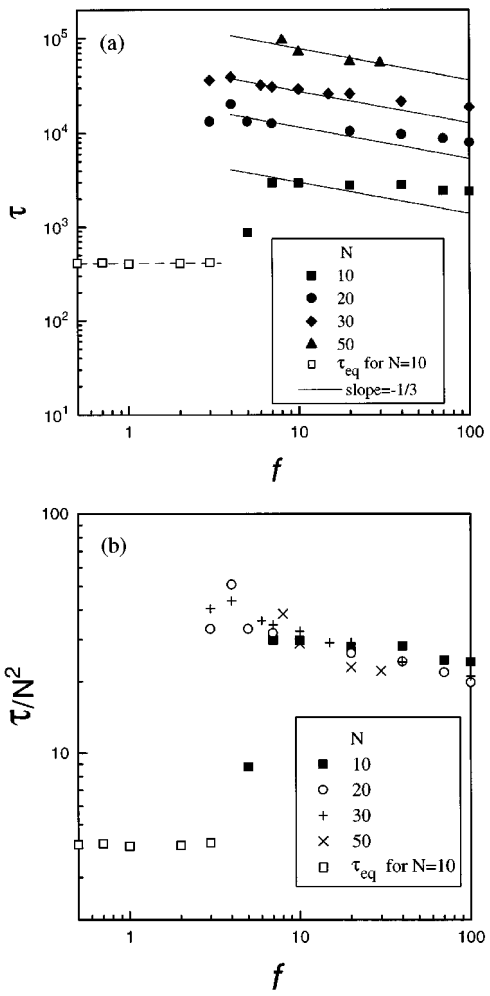

FIG. 10. (a) Monte Carlo data for the nonequilibrium relaxation time (in units of MCS/monomer) vs force for various chain lengths. (b) Same data as in (a) but plotted with τ/N^2 vs f.

and (20) is compared with our Monte Carlo data as shown in Fig. 10(b) for τ/N^2 vs f with various values of N. The data roughly collapse for f in the Pincus regime and beyond, hence suggesting the scaling $\tau \propto N^2$ is roughly correct.

This behavior of $\tau \sim N^2 f^{-2+1/\nu}$ in the Pincus regime can also be understood physically as follows: before releasing the chain, blobs form when the external force is large enough. It is also known that the blob size decreases as the force increases as f^{-1}. In the Pincus regime, the relaxation process is dominated by the rearrangement between blobs which contain undisturbed sections of the chain. With increasing force, the number of monomers inside a blob becomes less. Small blobs rearrange themselves more quickly than large blobs, thus resulting in a decrease in τ. A scaling description of the relaxation time before the chain is released can be formulated [25] based on the blob picture: Each blob has a relaxation time $\tau_{\rm blob} = \xi^2/D_{\rm blob} \propto \xi^2 g$, where g is the number of monomers inside a blob, $D_{\rm blob}$ is the corresponding diffusion constant. Similar to the motion of chains restricted to tubes, which also occurs in a stretched configuration $R_{gz} \sim \xi(N/g) \sim \xi^{1-1/\nu} N$, where ξ is the tube radius. Now the chain is released at $t=0$, the nonequilibrium relaxation time can be estimated from the time needed for density fluctuations to diffuse along the chain, $\tau \approx (N/g)^2 \tau_{\rm blob} \sim N^2 \xi^{2-1/\nu}$. Thus, in a good solvent regime, $\tau \sim N^2 \xi^{1/3}$. This expression supports our findings that, as the blob size decreases, the relaxation time decreases. Also, in the Pincus regime, $\xi \sim f^{-1}$, so $\tau \sim N^2 f^{-2+1/\nu}$. The results of this blob scaling analysis are consistent with our analysis through the mechanical energy balance in Sec. III B and our simulation data.

VII. DISCUSSIONS AND OUTLOOK

In this work, dynamic Monte Carlo simulation and scaling calculations were performed to investigate the static and dynamic behaviors of a single polymer chain under stretching forces in good solvents. The polymers were simulated in a continuous space using the bead-spring chain model. Our Monte Carlo results for the static quantities explicitly verified the scaling laws proposed by de Gennes and Pincus. These results agreed with other simulation works on lattices, thus explicitly verifying the universality behavior. It is again verified that, at weak stretching forces, the deformation of the chain obeys Hooke's law ($\langle R_f \rangle \sim f$), and for stronger forces the Pincus expression applies ($\langle R_f \rangle \sim f^{2/3}$). As a by product, our data for the lateral spread of the chain $\langle R^2_{\rm perp} \rangle$ were shown to scale as $f^{-1/3}$ in the Pincus regime, as predicted [10].

For nonequilibrium studies of the relaxation of a stretched chain, we were able to monitor the evolution of the averaged relaxation processes $\overline{R_{gz}(t)/R_{gz}(0)}$ as the external force was removed at $t=0$. Although the averaged $R_{gz}(t)$ decays monotonously, rebounds of $R_{gz}(t)$ were found for almost all of the relaxation processes. Snapshots of the configurations of the polymer chain were extracted from simulations during the relaxation processes. The resulting plots greatly resemble the experimental pictures shown in work by Perkins *et al.* We have also found that a certain time after the removal of the external force, a portion of the chain near the free end relaxes roughly to the unperturbed state, while other parts of the chain remain in different degrees of the stretched structures. This ''unperturbed'' portion of the chain moves quite freely in the neighborhood, and thus the end-to-end distance in the $\hat{z}$ direction fluctuates rather strongly. Sometimes this free end section coils into a ball shape and may correspond to the ''compact ball'' observed in experiments by Perkins *et al.* Such a chain configuration is in agreement of the ''stem and flower'' conformation [6] at intermediate times in the relaxation process. The ''stem and flower'' model predicts the nonequilibrium relaxation of the chain length scales as $R_f(0) - R_f(t) \propto \sqrt{t}$, which was also observed in a very recent experiment by Manneville *et al.* [26]. Our simulation results on $\overline{R_{gz}(t)/R_{gz}(0)}$ at sufficiently strong f indicate two important time-scale regimes for the relaxation of a nearly fully stretched polymer. In Fig. 11, a scaling plot of the dimensionless quantities $\overline{R_{gz}(t)/R_{gz}(0)}$ vs $t/\tau_{1/2}$ [where $R_f(\tau_{1/2}) = R_f(0)/2$] for various values of f is shown. In the earlier stage, the relaxation is primarily due to the movement of the free end, and our data are consistent with the prediction of the ''stem and flower'' model, namely, $\overline{R_{gz}(t)/R_{gz}(0)} = 1 - {\rm const} \times \sqrt{t}$ (the dashed line in Fig. 11). However, at longer times, the whole chain undergoes a re-

laxation behavior compatible with $R_f(t) \propto \exp(-t/\tau)$, where τ is the longest relaxation time. This is in agreement with the Rouse model, and also as observed by Perkins *et al.* [1]. It should be noted that the ''stem and flower'' relaxation behavior does not occur (and the $\sqrt{t}$ behavior is not observed in our data either) when the stretching force is not strong (such as the data for $f<20$ in Fig. 9). In this case, the chain is not close to its stretch limit, and the conformation of the chain is a string of blobs and thus the relaxation behavior is due to rearrangement of the blobs and hence $R_f(t) \propto \exp(-t/\tau)$ is observed.

The nonequilibrium relaxation time τ is extracted from the data of $\overline{R_{gz}(t)/R_{gz}(0)}$. We found that there are three regions: linear, Pincus, and model-dependent regions for different dynamic behaviors of the polymer chains. We also performed simple calculations for the nonequilibrium relaxation times based on the mechanical energy balance. The analysis indicates that in the linear regime the driving force for the relaxation process is the same as that in the equilibrium state and thus the relaxation times remain constant in this regime. Our scaling analysis also shows that in the Pincus regime there is a decrease in the nonequilibrium relaxation time as force increases ($\tau \sim f^{-1/3}$) in good solvents. These results are verified by our simulation data. Another scaling description based on the blob picture also supports our findings. In the ultrastrong-force model-dependent regime, we obtained a result for the nonequilibrium relaxation time using the freely jointed chain model. Unfortunately, there are no experiments on the dependence of τ on the force f to compare with our results. We hope that our results can stimulate future experiments on this issue.

On the other hand, our results for the nonequilibrium relaxation-time dependence on N can be compared with the findings in the experiment by Perkins *et al.* In this experiment, the polymer chain was stretched by flow to near its fully extended limit, and the flow was then stopped and the relaxation processes were observed. They found the scaling law $\tau \sim N^b$ for some exponent $b=1.53$–1.79 depending on the length of the chains. Our present study [Eq. (17)] gives $\tau \propto N^2$, the discrepancy may be due to the following reasons: (i) The DNA in the experiment is near its fully stretched limit and hence should be model dependent, one should not expect a universal scaling law of τ to hold. However, from our result using the freely jointed chain, one still has $\tau \propto N^2$ [Eq. (20)], thus it seems that the nonuniversal behavior may not be strong enough to account for the discrepancy. (ii) The DNA chain has a double-helix structure which may have a rather peculiar recoil mechanism from ordinary bead-spring-type polymer chain. (iii) The hydrodynamics of the solvent is absent in our analysis and Monte Carlo simulations. In the experiments, the solvent would give rise to complicated flow and backflow that could significantly affect the relaxation behavior. (iv) Hydrodynamic screening is also absent in both the simulation and analysis. The Monte Carlo simulation and the analysis in Sec. III basically obey the Rouse model in which all monomers experience the viscous damping and no screening of the type similar to the Zimm model is present. However, we believe that since the chain is in a rather stretched configuration in the experiment, such hydrodynamic screening should not be important. (v) Finally, the assumption in Eq. (14) that every monomer experiences the same viscous damping is not strictly valid. Since not all monomers will move with the same characteristic speed $\partial R_f/\partial t$, at least the monomer at the fixed end is immobile. Also monomers near the fixed end tend to move rather slowly. One can push this to the extreme limit if only the monomer in the free end experiences viscous damping and the rest of the monomers feel no drag (a very unrealistic case); then one easily finds $\tau \propto N$. The experimental situation is somewhere in between, and hence one can qualitatively account for the fact that the exponent b is between 1 and 2. The fact that the experimental value of b is 1.57–1.79, only somewhat less than 2, may suggest that the assumption in Eq. (14) is not too bad. To summarize, we believe that the discrepancy arises mainly due to combinations of (ii), (iii), and (v) from above.

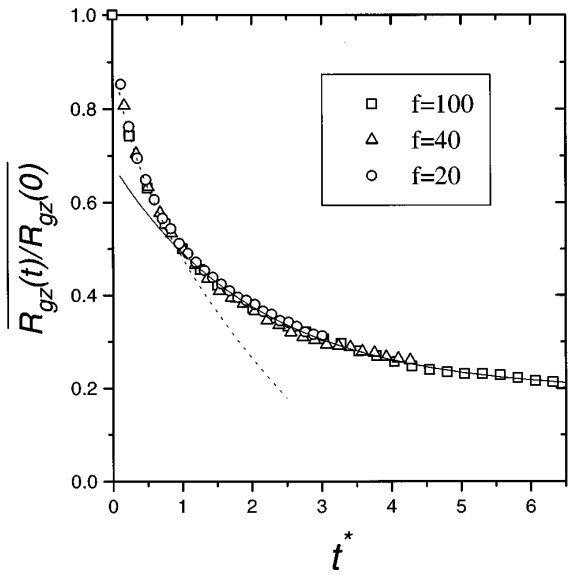

FIG. 11. $\overline{R_{gz}(t)/R_{gz}(0)}$ vs $t^* \equiv t/\tau_{1/2}$, where $R_{gz}(\tau_{1/2}) = R_{gz}(0)/2$ for $N=30$ under different stretching forces. The solid curve is an exponential decay fit and the dashed curve is a fitting of the prediction $1-\text{const} \times t^{1/2}$.

So far, we focused on studying the dynamic behavior of a single stretched polymer chain in good solvent conditions. Our approach can be readily extended to a study of the dynamical behaviors of the polymer chain in other conditions. For example, the nonequilibrium dynamics of a single polymer chain quenched to the poor solvent regime is of great importance both practically and theoretically. We also plan to investigate the topological effects on the force law in polymer systems. As we know, the self-crossing of the macromolecular sections are forbidden, and these nonphantom characteristics are especially important for the dynamic properties of chains of a nontrivial topology. Studies of polymer chains with a nontrivial topology can help clarify the essence of the topological problems in polymer physics.

ACKNOWLEDGMENTS

This research was supported by National Council of Science of Taiwan under Grant No. NSC 86-2112-M-008-013. Computing time provided by the Simulational Physics Laboratory, National Central University, is gratefully acknowledged.

[1] T. T. Perkins, S. T. Quake, D. E. Smith, and S. Chu, Science **264**, 822 (1994).
[2] T. T. Perkins, D. E. Smith, R. G. Larson, and S. Chu, Science **268**, 83 (1995).
[3] P. G. de Gennes, *Scaling Concepts in Polymer Physics* (Cornell University Press, Ithaca, NY, 1979).
[4] F. Brochard-Wyart, Europhys. Lett. **23**, 105 (1993).
[5] F. Brochard-Wyart, H. Hervet, and P. Pincus, Europhys. Lett. **26**, 511 (1994).
[6] F. Brochard-Wyart, Europhys. Lett. **30**, 387 (1995).
[7] P.-Y. Lai, Physica A **221**, 233 (1995).
[8] P.-Y. Lai, Phys. Rev. E **53**, 3819 (1996).
[9] P. G. de Gennes, Macromolecules **9**, 587 (1976).
[10] P. Pincus, Macromolecules **9**, 386 (1976).
[11] I. Webman, J. L. Lebowitz, and M. H. Kalos, Phys. Rev. A **23**, 316 (1981).
[12] M. Wittkop, J.-U. Sommer, S. Kreitmeier, and D. Goritz, Phys. Rev. E **49**, 5472 (1994).
[13] P. Pincus, Macromolecules **10**, 210 (1977).
[14] K. Binder and W. Paul, J. Polymer Sci. B **35**, 1 (1997).
[15] Y.-J. Sheng, A. Z. Panagiotopoulos, S. K. Kumar, and I. Szleifer, Macromolecules **27**, 400 (1994).
[16] Y.-J. Sheng, A. Z. Panagiotopoulos, and D. P. Tassios, AIChE. J. **41**, 2306 (1995).
[17] Y.-J. Sheng, A. Z. Panagiotopoulos, and S. K. Kumar, J. Chem. Phys. **103**, 10315 (1995).
[18] D. Frenkel, G. C. A. M. Mooij, and B. Smit, J. Phys. Condens. Matter. **4**, 3053 (1992).
[19] J. J. de Pablo, M. Laso, and U. W. Suter, J. Chem. Phys. **96**, 6157 (1992).
[20] M. P. Allen and D. J. Tildesley, *Computer Simulations of Liquids* (Oxford University Press, New York, 1987).
[21] W. Paul, K. Binder, K. Kremer, and D. W. Heermann, J. Chem. Phys. **95**, 7726 (1991).
[22] P.-Y. Lai, Phys. Rev. E **49**, 5420 (1994).
[23] I. Gerroff, A. Milchev, K. Binder, and W. Paul, J. Chem. Phys. **98**, 6526 (1993).
[24] S. B. Smith, L. Finizi, and C. Bustamante, Science **258**, 1122 (1992).
[25] P.-Y. Lai and K. Binder, J. Chem. Phys. **95**, 9288 (1991).
[26] S. Manneville, Ph. Cluzel, J.-L. Viovy, D. Chatenay, and F. Caron, Europhys. Lett. **36**, 413 (1996).